cosmetics

MDPI

Article

Deciphering the Phytochemical Profile of an Alpine Rose (*Rhododendron ferrugineum* L.) Leaf Extract for a Better Understanding of Its Senolytic and Skin-Rejuvenation Effects

Jane Hubert [1,*], Alexis Kotland [1], Bernhard Henes [2], Stéphane Poigny [2] and Franziska Wandrey [2]

[1] NatExplore SAS, 51140 Prouilly, France; alexis.kotland@nat-explore.com
[2] Mibelle Group Biochemistry, Mibelle AG, 5033 Buchs, Switzerland; bernhard.henes@mibellegroup.com (B.H.); stephane.poigny@mibellegroup.com (S.P.); franziska.wandrey@mibellegroup.com (F.W.)
* Correspondence: jane.hubert@nat-explore.com; Tel.: +33-6-19-02-75-06

Abstract: *Rhododendron ferrugineum*, commonly named Alpine rose, is an emblematic medicinal plant of European mountains. In this study, the chemical profile of a glycerol/water extract developed from this plant as a cosmetic ingredient is investigated to understand the extract constituent(s) that could mostly contribute to its senolytic activity and skin-rejuvenation effects. For this purpose, the dereplication method "CARAMEL", which combines Centrifugal Partition Chromatography to Nuclear Magnetic Resonance data interpretation, was directly applied to the hydro-glycerinated extract, leading to the unambiguous identification of fourteen Alpine rose metabolites, despite the strong presence of the heavy solvent glycerol. Flavonoids derived from taxifolin, quercetin, and (+)-catechin were identified as significant constituents of the extract, followed by flavanones, orcinol derivatives, phloroacetophenone, and phenolic acids, as well as the pentacyclic triterpene lupeol. Given that senolytic molecules are known to selectively induce the death of senescent cells without affecting healthy proliferating cells, which can be achieved by the selective inhibition or downregulation of the anti-apoptotic Bcl-2 protein, and considering the well-recognized pro-apoptotic activity of hyperoside, taxifolin, naringenin and farrerol, the senolytic activity of the glycerol/water Alpine rose extract can be explained by the abundance of flavonoids present in the extract.

Keywords: *Rhododendron ferrugineum*; natural cosmetics; senolytic activity; skin rejuvenation; NMR-based dereplication; LC/MS chemical profiling; glycerol extract; flavonoids

Citation: Hubert, J.; Kotland, A.; Henes, B.; Poigny, S.; Wandrey, F. Deciphering the Phytochemical Profile of an Alpine Rose (*Rhododendron ferrugineum* L.) Leaf Extract for a Better Understanding of Its Senolytic and Skin-Rejuvenation Effects. *Cosmetics* **2022**, *9*, 37. https://doi.org/10.3390/cosmetics9020037

Academic Editor: Enzo Berardesca

Received: 7 March 2022
Accepted: 22 March 2022
Published: 24 March 2022

1. Introduction

Rhododendron ferrugineum L. (Ericaceae), commonly named Alpine rose, is an evergreen subalpine shrub growing throughout the European mountains at elevations between 1700 and 2300 m. It can be highly abundant in some parts of the northwestern Alps, where it outcompetes other plants and extensively colonizes grazed or abandoned meadows [1,2]. This plant is well adapted to extreme environmental conditions and has developed specific morphological and phytochemical characteristics. The leaves accumulate, for instance, specific proteins called dehydrins, which can protect against UV radiations and help to survive periods of frost and drought [3].

In Germany and Switzerland, *Rhododendron ferrugineum* is a very popular medicinal plant. Decoctions of the leaves have been traditionally used to treat rheumatism or blood pressure. An antiviral activity against Herpes simplex virus I has also been reported for an aqueous extract obtained from the aerial parts [4], as well as an inhibitory activity against *Porphyromonas gingivalis* adhesion to epithelial buccal KB cells for an aqueous extract obtained from the leaves, suggesting an antimicrobial potential in the prevention of periodontal diseases [5].

In recent years, *Rhododendron ferrugineum* was also used to develop active ingredients with cosmeceutical applications [6]. More specifically, it was recently shown that an Alpine

rose glycerol/water extract obtained from the leaves can eliminate senescent cells from the skin [7]. Treatment of normal human dermal fibroblasts with this extract reduced the number of senescent cells, while not affecting normal proliferating cells, similarly to the known senolytic drug Navitoclax. The efficacy of the extract was also demonstrated in a double-blind, placebo-controlled trial by significantly decreasing skin redness and increasing skin elasticity when applied topically at 2% in an emulsion [7]. As senescent cells greatly contribute to skin aging by inducing and accelerating inflammatory reactions and degradation of extracellular matrix, these previous results suggest a great potential of *Rhododendron ferrugineum* leaves in skin rejuvenation processes.

From a phytochemistry point of view, *Rhododendron ferrugineum* is known to contain a diversity of phenolic compounds, including flavonoids derived from quercetin, kaempferol and myricetin, dihydroflavonol glycosides mainly derived from taxifolin, as well as phloracetophenones [8,9]. A range of pentacyclic triterpenes, orsellinic acid derivatives, coumarins, such as scopoletin, and ferruginenes were also reported in a biologically active chloroform extract of *Rhododendron ferrugineum* leaves [10]. This extract displayed a cytotoxic activity against human promyelocytic leukemia HL-60 cells [11].

In the present study, the chemical profile of the active glycerol/water extract obtained from *Rhododendron ferrugineum* leaves is investigated to tentatively understand the metabolite(s) that might contribute most effectively to the senolytic activity of the whole extract. The identification strategy is based on a dereplication method organized in four steps and named CARAMEL (CARActérisation de MELanges in French, for mixture characterization) [12]. The workflow starts by the liquid–liquid fractionation of the crude extract, then Nuclear Magnetic Resonance (NMR) analysis of the produced fraction series, followed by the organization and visualization of the whole NMR dataset with the help of Hierarchical Clustering Analysis (HCA), and finally by searching a natural metabolite database in which metabolite(s) can be assigned to the NMR chemical shift cluster(s) obtained by HCA. The CARAMEL dereplication workflow enables the quick attainment of a global and detailed view of the chemical profile of natural extracts without discrimination between chemical classes, and without any loss of biomass, which means that 100% of the starting extract mass can be recovered at the end of the identification process under the form of a well-characterized fraction series. The efficiency of this ^{13}C NMR-based identification workflow has been demonstrated in many previous phytochemical investigations of various extracts of natural origin, including terrestrial plants, micro- and macroalgae, and cultured cell extracts of plant or microbial origin [13–17]. The method is adapted in the present study for the Alpine rose extract, which was developed in a solvent mixture containing 50% (*w/w*) of glycerol having a high boiling point, and thus could not be easily eliminated by usual low-pressure evaporation. The obtained chemical profile was exploited and compared to the literature data to tentatively correlate the presence of specific metabolite(s) to the skin-rejuvenation effects of the extract.

2. Materials and Methods

2.1. Plant Extract, Chemicals, and Solvents

Ethyl acetate, acetonitrile, and methanol (MeOH) were purchased from Carlo Erba (Val de Reuil, France). Acetic acid and formic acid were purchased from VWR (Radnor, PA, USA). Deionized water was used to prepare all the aqueous solutions. An Ecocert certified glycerol/water extract (1/1, *w/w*) obtained from the leaves of *Rhododendron ferrugineum* cultivated in the Swiss Alps was provided by Mibelle Group Biochemistry (Buchs, Switzerland). *Rhododendron ferrugineum* leaves were manually collected from a wild harvesting place respecting the organic label "bioknospe", which guarantees a pesticide-free biomass. The leaves are regenerated in the following year, ensuring sustainability. To obtain the extract, 2% (*w/w*) of *Rhododendron ferrugineum* leaves were cut down (Retsch Schneidmühle SM 100) and extracted in a flow-through extractor system (Dig-Maz 100) for 5 h at 55 °C with glycerol/water (1/1, *w/w*).

2.2. Extract Fractionation by Centrifugal Partition Chromatography

The glycerol/water extract (1/1, *w/w*) was preliminarily evaporated under vacuum with a rotary evaporator at 50 °C, 5 mbar during 5 h to eliminate water. A concentrated extract of 76 g was obtained from 150 g of the starting sample. This concentrated extract was fractionated by Centrifugal Partition Chromatography (CPC) over 2 strictly identical experiments, each starting from 33 g (total mass used for CPC = 66 g). CPC was performed with an FCPE300® (Rousselet Robatel Kromaton). A column with a 303 mL capacity was made of 7 partition disks engraved with 231 twin cells of ≈1 mL each. The liquid phases were pumped with a Knauer preparative 1800 V7115 pump. The biphasic solvent system was ethyl acetate/acetonitrile/water (3/3/4, *v/v*) used in the ascending mode, and the flow rate was set at 20 mL/min. After filling the column with the lower phase of the biphasic solvent system, and equilibration at 1300 rpm and 20 mL/min, the glycerol concentrated extract was diluted in 10 mL of water + 6 mL of acetonitrile and injected. The mobile phase (upper phase) was pumped for 64 min for the elution step. Then, all the compounds retained inside the column were recovered by extrusion for 10 min. Fractions of 20 mL were collected over the whole experiment (elution and extrusion) and combined according to their thin-layer chromatography profiles (TLC). TLC was performed with a CAMAG® automatic sampler ATS4, a CAMAG® automatic developing chamber ADC2, and a CAMAG® TLC visualizer 2. Fractions were deposited on pre-coated silica gel 60 F_{254} Merck plates with the migration solvent system ethyl acetate/acetic acid/formic acid (10/1/1, *v/v*), visualized under UV light 254 nm and 366 nm, and revealed by spraying the dried plates with 50% H_2SO_4 and vanillin followed by heating. As a result, 10 identical final fractions accumulated from the 2 CPC experiments were obtained (Figure 1). The mass distribution of all the fractions is also indicated in Figure 1.

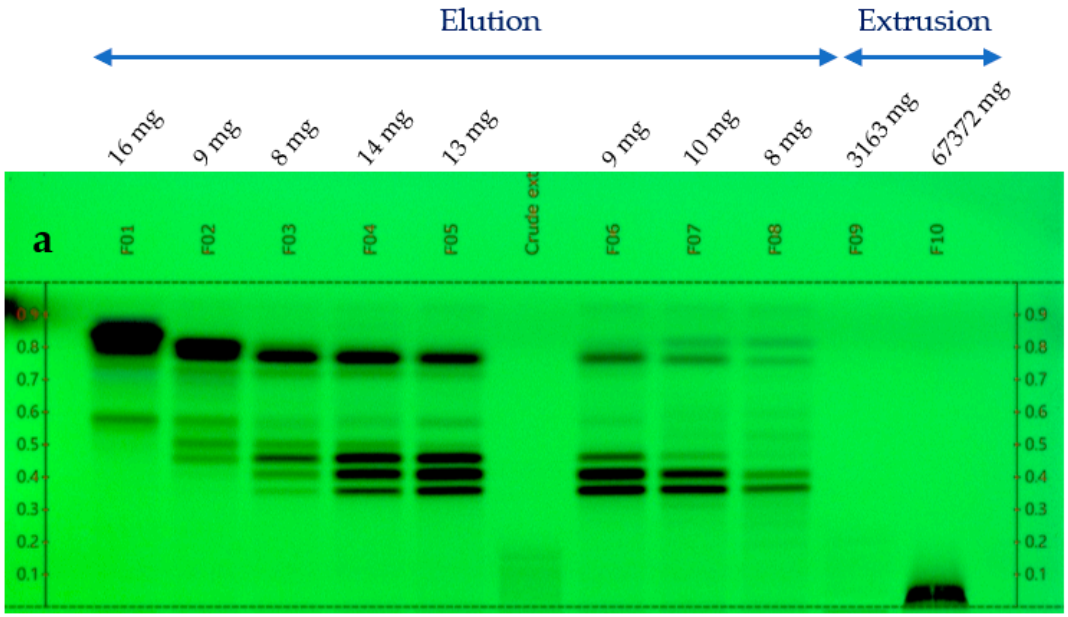

Figure 1. *Cont.*

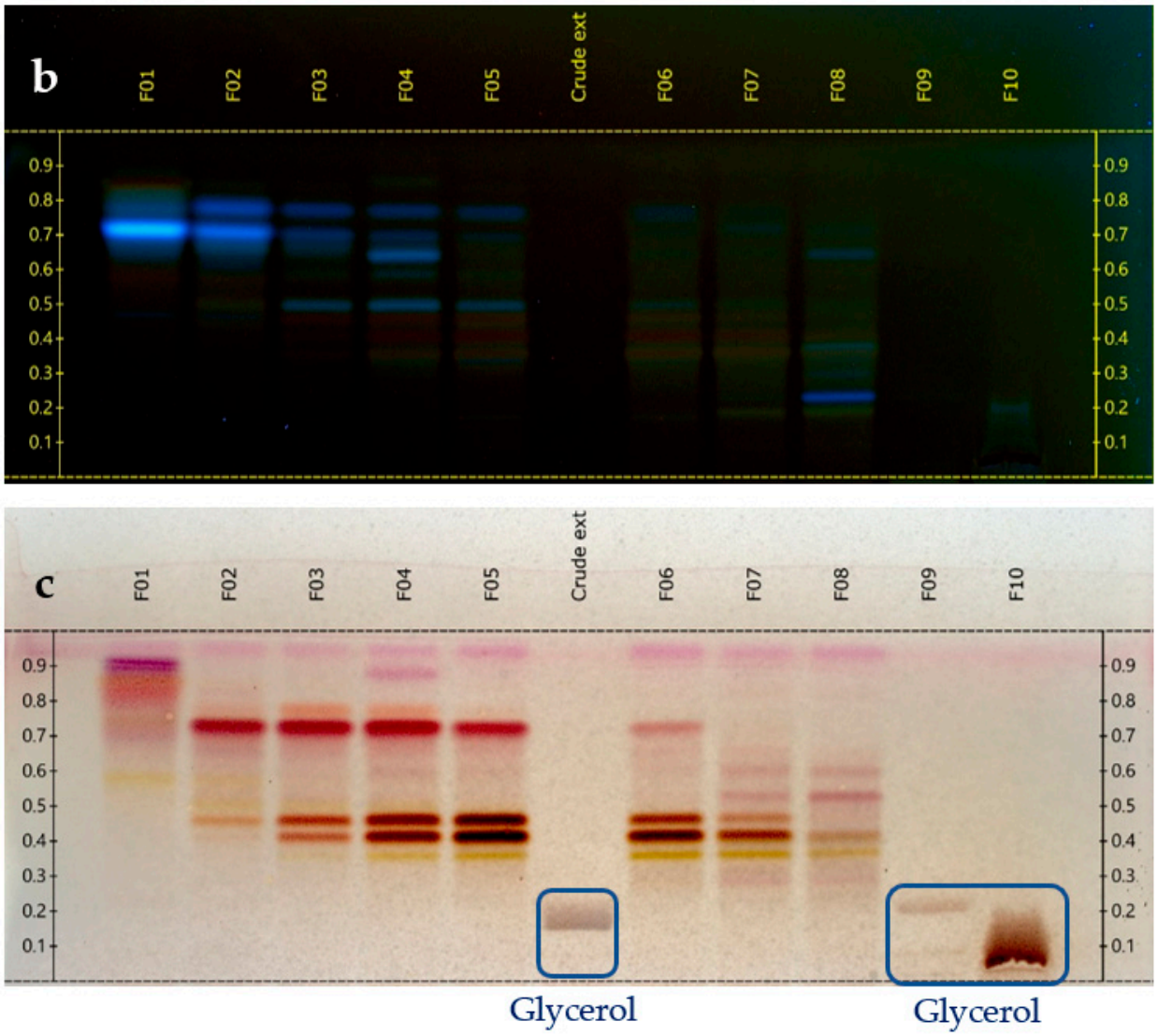

Figure 1. TLC profile of the 10 CPC fractions. (**a**) 254 nm; (**b**) 366 nm; and (**c**) visible after vanillin/H_2SO_4 reagent spraying and heating.

2.3. NMR Analyses and Identification of the Alpine Rose Extract Constituents by CARAMEL

An aliquot of each fraction from F1 to F10 (up to 20 mg, when possible) was dissolved in 600 µL of DMSO-*d6* and analyzed by NMR at 298 K on a Bruker Avance AVIII-600 spectrometer (Karlsruhe, Germany) equipped with a cryoprobe optimized for ^{1}H detection and with cooled ^{1}H, ^{13}C, and ^{2}H coils and preamplifiers. ^{13}C NMR spectra were recorded using the UDEFT sequence with an acquisition time of 0.36 s, a relaxation delay of 3 s. A total of 512 scans were co-added to obtain a satisfactory signal-to-noise ratio. The spectral width was 240 ppm and the receiver gain was set to the highest possible value. Spectra were then manually phased and baseline corrected using the TopSpin 4.0.5 software from Bruker. The central resonance of DMSO-*d6* was set at 39.8 ppm for spectrum calibration. All fractions were also analyzed with the zg (^{1}H), HSQC (^{1}H-^{13}C single-bond correlations), HMBC (^{1}H-^{13}C indirect correlations between carbons and protons separated by two, three, or four bonds), and COSY (^{1}H-^{1}H correlations between protons on neighboring carbons) sequences using standard Bruker parameters. For the CARAMEL identification process, all the detectable peaks of the ^{13}C NMR spectra of all fractions were automatically collected and exported as text files, from which the peak chemical shifts and their absolute intensities were submitted to bucketing using a locally developed computer script written in Python (bucket size = 0.3 ppm). The resulting table was imported into the PermutMatrix software

(version 1.9.3, LIRMM, Montpellier, France) for Hierarchical Clustering Analysis. Because the ^{13}C NMR spectra of fractions F09 and F10 only exhibited intense NMR signals of glycerol (Figure 2), these two spectra were removed from the dataset submitted to HCA, thus only fractions F01–F08 were included in the identification process. The clusters of chemical shifts organized on the resulting HCA heat map (Figure 3) were submitted to an in-house database comprising the structures and calculated chemical shifts of natural products (≈7000 entries in February 2022). NMR chemical-shift predictions were performed using the NMR Workbook Suite 2012 software from ACD/Labs (Ontario, Canada). Finally, the chemical structures proposed by the database were confirmed or further completed by an interpretation of 2D NMR data.

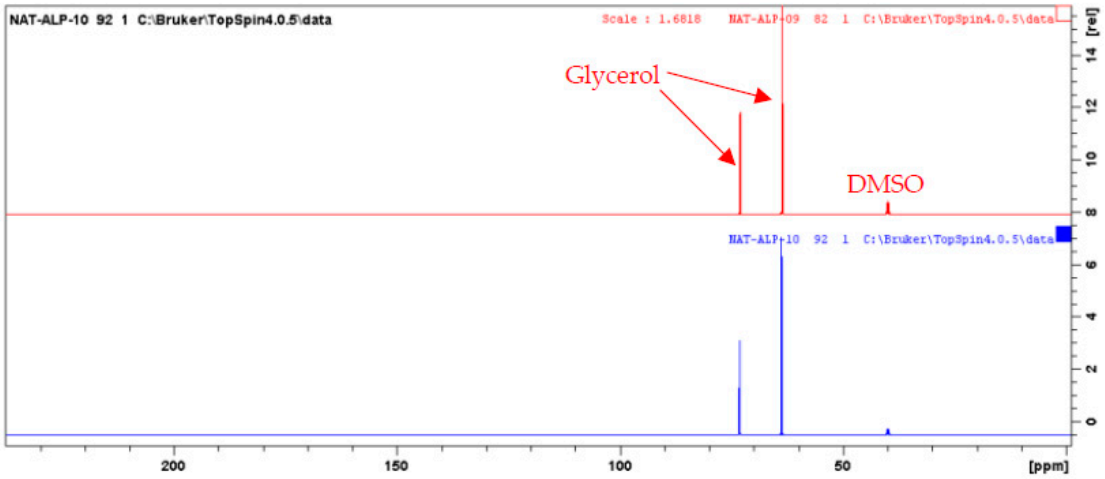

Figure 2. ^{13}C NMR spectra of CPC fractions F09 and F10.

2.4. LC/MS Analyses

The concentrated Alpine rose extract was also analyzed by high resolution LC/MS with an Acquity UPLC H-Class (Waters, Manchester, UK) system coupled to a Synapt G2-Si from Waters equipped with an electrospray (ESI) ion source. The chromatographic column was an Uptisphere C-18 ODB 150 * 4.6 mm, 5 µm from Interchim, maintained at 35 °C. The mobile phase gradient started with 100% solvent A (MilliQ water + 0.1% formic acid) and 0% solvent B (acetonitrile + 0.1% formic acid), then increased to 26% solvent B in 4 min, to 65% solvent B from 4 to 18.5 min, to 100% solvent B at 18.7 min, remained at 100% solvent B for 5 min, and then recycled back to 100% solvent A from 23.7 to 23.9 min and remained at 100% solvent A until 26 min. The flow rate was set at 0.7 mL/min and the sample injection volume was 1 µL. The MS acquisition was performed in the negative-ion mode within the scan range $50 < m/z < 2000$. The capillary voltage was set at 2 kV, the desolvation temperature at 450 °C, the desolvation gas flow at 950 L/h, the source temperature at 120 °C, the cone voltage at 40 V, and the cone gas flow at 50 L/h. Data were processed using the MassLynx software from Waters.

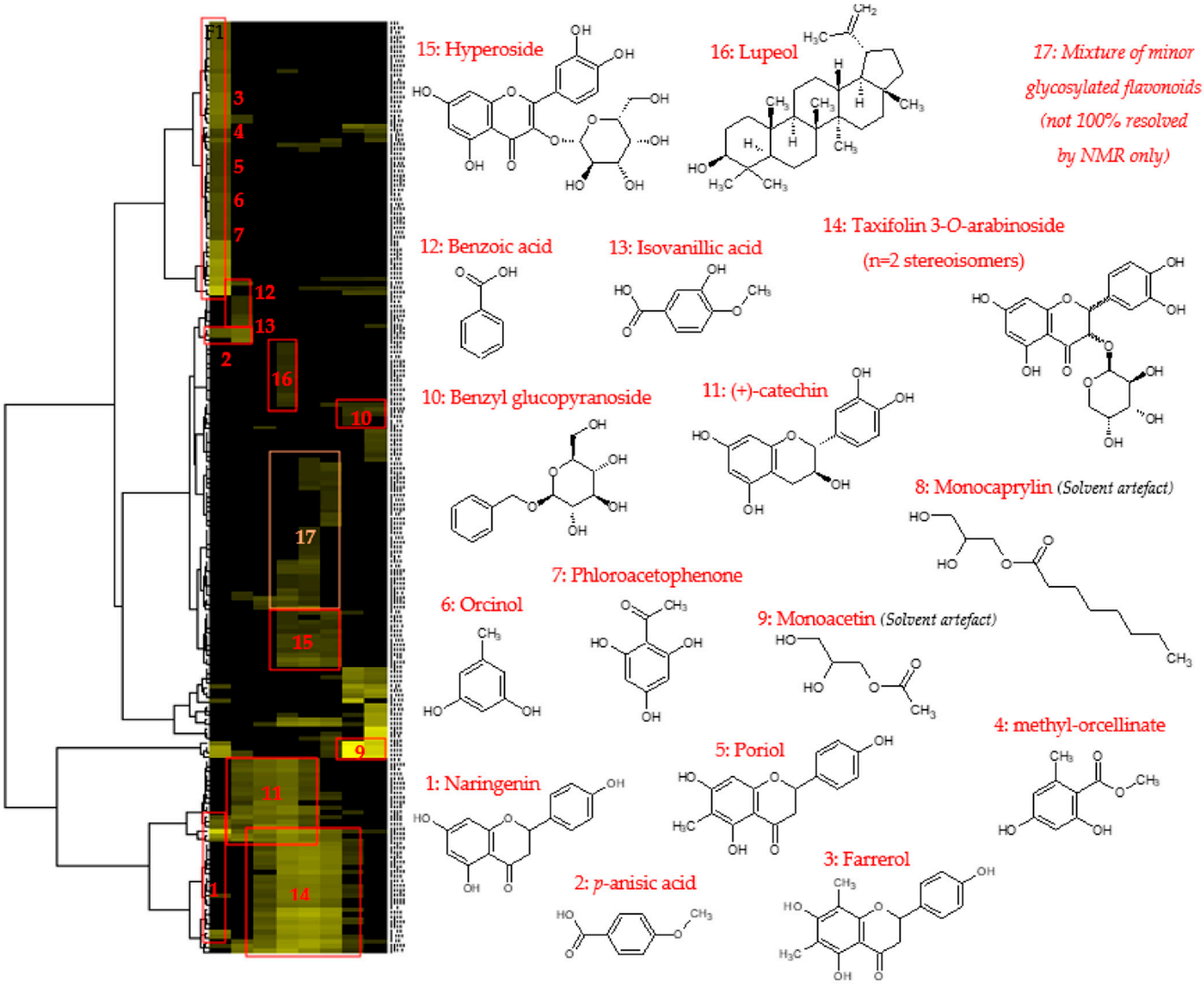

Figure 3. HCA correlation map of ^{13}C NMR signals with the identified compounds.

3. Results and Discussion

The Alpine rose extract examined in this study was previously reported to have a senolytic activity on senescent fibroblasts, and to significantly reduce redness and increase skin elasticity in a placebo-controlled clinical study [6]. The objective in the present study was to tentatively understand the extract constituent(s) that could mostly contribute to these anti-aging effects. The active extract was developed in an industrial context from the leaves of the plant species *Rhododenron ferrugineum* using a glycerol/water (1/1, *w/w*) mixture as an extraction and stabilization solvent. Natural extracts of industrial interest for the development of cosmetic ingredients are, nowadays, commonly prepared or stabilized in matrices that contain glycerol. Glycerol has the advantages of being nontoxic, biodegradable, renewable, largely available, cost effective, completely miscible with water, colorless, and of low volatility with a vapor pressure of 0.000106 hPa at 25 °C [18].

At the same time, the high boiling point of glycerol makes it difficult to eliminate by a simple evaporation, and thus represents a great barrier for the chemical analysis of natural extracts, which are stabilized in such matrices. Therefore, one challenge of this work was to establish the chemical profile of this glycerol/water (1/1, *w/w*) Alpine rose extract, as precisely as possible. The selected strategy was to separate glycerol from the Alpine rose extract constituents by Centrifugal Partition Chromatography using a quite polar biphasic solvent system composed of ethyl acetate, acetonitrile, and water in the proportions of

3/3/4 (*v*/*v*). This biphasic solvent system was previously reported to be stable in the presence of glycerol and able to separate compounds within a wide polarity range [19]. Our objective during the fractionation of the Alpine rose extract was to retain the glycerol in the stationary phase of the CPC column, as much as possible, while eluting the Alpine rose compounds of interest. As illustrated on the TLC profiles in Figure 1, fractions F01–F08 recovered from the elution step represented only 87 mg of biomass, but exhibited a high chemical diversity with several metabolites fluorescing at 254 nm and 360 nm, probably corresponding to the specialized metabolites of *Rhododendron ferrugineum*. The yellow stains observed under visible light after chemical revelation with H_2SO_4 and vanillin indicate the presence of flavonoids. At the end of the CPC fractionation, glycerol was only contained in fractions F09 and F10, suggesting that the CARAMEL identification procedure could be successfully applied on the fraction series F01–F08. It must be noted that the fractions F09 and F10 retained in the aqueous stationary phase also probably contained highly polar metabolites from *Rhododendron ferrugineum* leaves, such as sugars or amino acids. The NMR identification of these highly polar extract constituents was unfortunately not possible, due to the high amount of glycerol in F09 and F10, as illustrated in Figure 2. Therefore, the two spectra were removed from the dataset submitted to HCA, and only fractions F01–F08 were included in the identification process.

After 1D and 2D NMR analyses, an automatic peak picking was performed on ^{13}C NMR spectra of fractions F01–F08, and the collected peaks were aligned across the fraction series using a bucketing strategy. The resulting table was made of eight columns corresponding to the CPC fractions, and 205 rows corresponding to the chemical shift buckets, for which at least 1 ^{13}C peak was detected in at least 1 fraction. The variables inside the table corresponded to the absolute intensities of ^{13}C NMR peaks. Hierarchical Clustering Analysis (HCA) was applied on the rows to organize ^{13}C NMR chemical shifts as clusters for the peaks having an identical evolution across the fraction series, probably meaning that these peaks belong to the same chemical structure. The HCA heat map is presented in Figure 3. Seventeen chemical shift clusters were aggregated on the heat map. These chemical shift clusters were tentatively assigned to chemical structures using a database that contains the predicted ^{13}C NMR chemical shifts of small natural metabolites. The chemical structures proposed by the database were then rigorously confirmed for all atom positions by 2D NMR data interpretation, leading to the unambiguous identification of a total of fourteen metabolites of the Alpine rose extract, as well as two compounds probably resulting from solvent artefacts (monoacetin and monocaprylin). Flavonoids were, by far, the main compounds detected in fractions F01–F08, with taxifolin 3-*O*-arabinoside as the leading representative of this chemical class, identified in fractions F03 to F07 under two stereoisomeric forms. Hyperoside and (+)-catechin were also significant constituents of the extract, followed by a diversity of flavanones, including naringenin, porriol, and farrerol. Orcinol, methyl-orcellinate, and phloroacetophenone were detected in the least fraction F01, followed by benzoic acid and isovanillic acid in fraction F02. One pentacyclic triterpene, namely, lupeol, was also identified in fraction F04. Glycosylated flavonoids, monomeric flavanols (catechin), and phloroacetophenone derivatives have already been reported in the leaves of *Rhododendron ferrugineum* [8,9,20]. The ^{13}C and ^{1}H NMR chemical shifts observed for all the fourteen identified metabolites and validated with the help of HSQC, HMBC, and COSY spectra of the CPC fractions are summarized in a Supplementary Data file.

High resolution LC/MS analysis of the starting extract in the negative ion mode also confirmed flavonoids derived from quercetin, taxifolin, and (+)-catechin as significant extract constituents (Figure 4 and Table 1). In addition to the NMR results, quinic acid, saccharose, citric acid, free taxifolin, quercetin rhamnoside and quercetin pentoside, monocaffeoylquinic acid, (−)-epicatechin, coumaric acid hexoside, cinnamic acid hexoside, and dihydrofarrerol were putatively identified by LC/MS based on exact mass measurement and formula annotation.

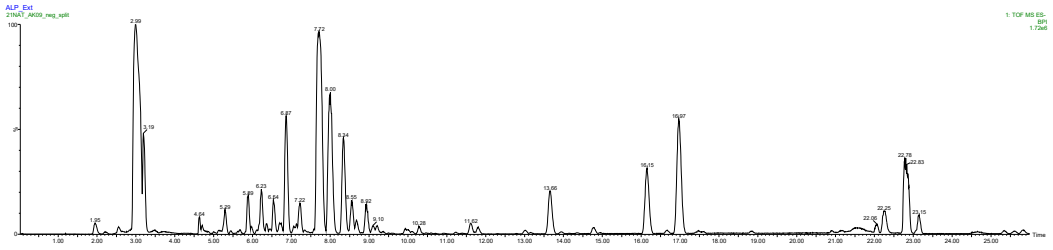

Figure 4. LC/MS chromatogram (BPI) of the glycerol/water Alpine rose extract—negative ion mode—ESI source.

Table 1. Summary of LC/MS data.

LC Retention Time (min)	Observed *m*/*z*	Elemental Composition	Δppm	Tentative Identification
2.92	191.0555 $[M-H]^-$	$C_7H_{11}O_6$	0.0	Quinic acid
3.21	341.1086 $[M-H]^-$	$C_{12}H_{21}O_{11}$	0.6	Saccharose
4.63	337.0769 407.1183	$C_{12}H_{17}O_{11}$ $C_{16}H_{23}O_{12}$	−0.6 −1.7	*Not assigned*
4.69	191.0191 $[M-H]^-$ 111.0082	$C_6H_7O_7$ $C_5H_3O_3$	−0.5 0.0	Citric acid
5.29	435.1143	$C_{17}H_{23}O_{13}$	0.9	*Not assigned*
5.44	329.0873 301.0559	$C_{14}H_{17}O_9$ $C_{12}H_{13}O_9$	0.0 −0.3	*Not assigned*
5.88	417.1030	$C_{17}H_{21}O_{12}$	−0.7	Kaempferol pentoside
6.22	329.0872	$C_{14}H_{17}O_9$	−0.3	Vanillic hexoside
6.36	227.0553	$C_{10}H_{11}O_6$	−1.3	Not assigned
6.55	417.1033	$C_{17}H_{21}O_{12}$	0.0	Kaempferol pentoside isomer
6.72	353.0876 $[M-H]^-$ 191.0557 quinic acid	$C_{16}H_{17}O_9$ $C_7H_{11}O_6$	0.8 0.5	Mono-caffeoylquinic acid
6.86	289.0717 $[M-H]^-$	$C_{15}H_{13}O_6$	1.7	(+)-catechin *
7.22	289.0714 $[M-H]^-$ 327.1079	$C_{15}H_{13}O_6$ $C_{15}H_{19}O_8$	0.7 −0.3	(−)-Epicatechin Coumaric acid hexoside
7.64	435.0934 $[M-H]^-$ 285.0401	$C_{20}H_{19}O_{11}$ $C_{15}H_9O_6$	1.6 0.7	Taxifolin 3-*O*-arabinoside isomer 1 *
7.98	463.0882 $[M-H]^-$	$C_{21}H_{19}O_{12}$	1.1	Hyperoside *
8.39	435.0928 $[M-H]^-$ 285.0399	$C_{20}H_{19}O_{11}$ $C_{15}H_9O_6$	0.2 0.0	Taxifolin 3-*O*-arabinoside isomer 2 *
8.53	433.0767 $[M-H]^-$	$C_{20}H_{17}O_{11}$	−0.9	Quercetin xyloside or arabinoside
8.67	447.0924 $[M-H]^-$	$C_{21}H_{19}O_{11}$	−0.7	Quercetin rhamnoside
8.92	505.0986 $[M-H]^-$ 301.0341 Quercetin	$C_{23}H_{21}O13$	0.8	Quercetin acetyl-hexoside
9.10	303.0501 $[M-H]^-$ 285.0397 $[M-H-H_2O]^-$	$C_{15}H_{11}O_7$ $C_{15}H_9O_6$	−1.3 −0.7	Taxifolin

Table 1. *Cont.*

LC Retention Time (min)	Observed *m/z*	Elemental Composition	Δppm	Tentative Identification
9.20	149.0601 311.1129 $[M-H]^-$	$C_9H_9O_2$ $C_{15}H_{19}O_7$	−1.3 −0.6	Cinnamic acid hexoside
9.92	167.0345 $[M-H]^-$	$C_8H_7O_4$	0.6	Isovanillic acid *
10.27	455.1551	$C_{21}H_{27}O_{11}$	−0.4	*Not assigned*
11.61	567.1141	$C_{21}H_{27}O_{18}$	−9.9	*Not assigned*
13.65	271.0606 $[M-H]^-$	$C_{15}H_{11}O_5$	0.0	Naringenin *
14.76	285.0760 $[M-H]^-$	$C_{16}H_{13}O_5$	−1.1	Poriol * or isomer
16.13	285.0763 $[M-H]^-$	$C_{16}H_{13}O_5$	0.0	Poriol * or isomer
16.96	299.0921 $[M-H]^-$	$C_{17}H_{15}O_5$	0.7	Farrerol *
16.63	297.0762 $[M-H]^-$	$C_{17}H_{13}O_5$	−0.3	Dihydrofarrerol

* also identified by NMR.

Considering the previously reported senolytic activity of the glycerol/water (1/1, *w/w*) Alpine rose extract, there are several candidate molecules identified in this study that could be responsible for this activity. Senolytics are molecules that selectively induce the death of senescent cells whilst not affecting healthy, proliferating cells, which leads to an increase in lifespan in many organisms [21]. This can be achieved through different mechanisms; the best described is by inducing apoptosis through the inhibition or downregulation of Bcl-2, which has been described to be responsible for apoptosis resistance in senescent cells as well as in cancer cells [22]. Hyperoside (Figure 3, 15), significantly present in the glycerol/water (1/1, *w/w*) Alpine rose extract has previously been shown to reduce Bcl-2 levels and induce apoptosis in breast cancer cells, and the docking of hyperoside to Bcl-2 has been modeled in silico [23,24]. Furthermore, naringenin (Figure 3, 1) as well as farrerol (Figure 3, 3) have also been previously described to induce apoptosis and reduce Bcl-2 expression in different cancer cell lines [25,26]. The treatment of different colorectal cancer cell lines with taxifolin decreased Bcl-2 levels and concomitantly increased the expression of the pro-apoptotic factor Bax [27]. Taken together, the senolytic activity of the glycerol/water (1/1, *w/w*) Alpine rose extract can be explained by the abundance of flavonoids present in the extract, for which senolytic activity has previously been suggested. Recently, skin senescence has been described to be a potent driver for the aging of the whole body [28]. Therefore, identifying ingredients suitable for topical application and targeting senescent skin cells, such as the Alpine rose extract investigated in this study, are of high interest in the cosmetic field and beyond.

4. Conclusions

The chemical profile of a glycerol/water extract obtained from the leaves of the Alpine rose (*Rhododendron ferrugineum*) was thoroughly examined using the ^{13}C NMR-based "CARAMEL" dereplication procedure, leading to the unambiguous identification of fourteen specialized metabolites. Flavonoids were the predominant phenolic constituents of the extract, and, among them, particular attention was given to hyperoside, naringenin, farrerol, and taxifolin, which were highlighted as the most probable constituents involved in the senolytic and skin-rejuvenation effects of the whole extract.

Supplementary Materials: The following supporting information can be downloaded at: https://www.mdpi.com/article/10.3390/cosmetics9020037/s1.

Author Contributions: Each author has made substantial contributions to the conception of the study, data acquisition and interpretation, and draft preparation. Individual contributions are distributed as follows: Conceptualization, J.H., S.P. and F.W.; Methodology, J.H., A.K. and B.H.; Software, J.H. and

A.K.; Writing—Original Draft Preparation, J.H., S.P. and F.W.; Writing—Review and Editing, J.H. and S.P.; Supervision, S.P., B.H. and F.W.; Project Administration, S.P., B.H. and F.W. All authors have read and agreed to the published version of the manuscript.

Funding: This research received no external funding.

Institutional Review Board Statement: Not applicable.

Informed Consent Statement: Not applicable.

Data Availability Statement: Not applicable.

Acknowledgments: This research was financially supported by Mibelle Group Biochemistry.

Conflicts of Interest: The authors declare no conflict of interest.

References

1. Francon, L.; Corona, C.; Till-Bottraud, I.; Choler, P.; Carlson, B.Z.; Charrier, G.; Améglio, T.; Morin, S.; Eckert, N.; Roussel, E.; et al. Assessing the effects of earlier snow melt-out on alpine shrub growth: The sooner the better? *Ecol. Indic.* **2020**, *115*, 106455.
2. Francon, L.; Corona, C.; Roussel, E.; Lopez Saez, J.; Stoffel, M. Warm summers, and moderate winter precipitation boost *Rhododendron ferrugineum* L. growth in the Taillefer massif (French Alps). *Sci. Total Environ.* **2017**, *586*, 1020–1031. [PubMed]
3. Wei, H.; Yang, Y.; Himmel, M.; Tucker, M.P.; Ding, S.Y.; Yang, S.; Arora, R. Identification and characterization of five cold stress-related rhododendron dehydrin genes: Spotlight on a FSK-Type dehydrin with multiple F-Segments. *Front. Bioeng. Biotechnol.* **2019**, *7*, 30. [PubMed]
4. Gescher, K.; Kühn, J.; Hafezi, W.; Louis, A.; Derksen, A.; Deters, A.; Lorentzen, E.; Hensel, A. Inhibition of viral adsorption and penetration by an aqueous extract from *Rhododendron ferrugineum* L. as antiviral principle against herpes simplex virus type-1. *Fitoterapia* **2011**, *82*, 408–413. [PubMed]
5. Löhr, G.; Beikler, T.; Hensel, A. Inhibition of *in vitro* adhesion and virulence of *Porphyromonas gingivalis* by aqueous extract and polysaccharides from *Rhododendron ferrugineum* L. A new way for prophylaxis of periodontitis? *Fitoterapia* **2015**, *107*, 105–113.
6. Cosmetics Design Europe. Available online: https://www.cosmeticsdesign-europe.com/Product-innovations/Ecocert-Certified-Alpine-Rose-Active-Combats-Aging-by-Protecting-Skin-Proteins (accessed on 5 February 2022).
7. Wandrey, F.; Schmid, D.; Zülli, F. Senolytics: Eliminating «zombie cells» in the skin—A novel anti-aging mechanism to combat senescent cells. *Ski. Care HPC Today* **2020**, *15*, 18–20.
8. Chosson, E.; Chaboud, A.; Chulia, A.J.; Raynaud, J. Dihydroflavonol glycosides from *Rhododendron ferrugineum*. *Phytochemistry* **1998**, *49*, 1431–1433.
9. Chosson, E.; Chaboud, A.; Chulia, A.J.; Raynaud, J. A phloracetophenone glucoside from *Rhododendron ferrugineum*. *Phytochemistry* **1998**, *47*, 87–88.
10. Popescu, R.; Kopp, B. The genus *Rhododendron*: An ethnopharmacological and toxicological review. *J. Ethnopharmacol.* **2013**, *147*, 42–62.
11. Seephonkai, P.; Popescu, R.; Zehl, M.; Krupitza, G.; Urban, E.; Kopp, B. Ferruginenes A–C from *Rhododendron ferrugineum* and their cytotoxic evaluation. *J. Nat. Prod.* **2011**, *74*, 712–717. [PubMed]
12. Hubert, J.; Nuzillard, J.M.; Purson, S.; Hamzaoui, M.; Borie, N.; Reynaud, R.; Renault, J.H. Identification of natural metabolites in mixture: A pattern recognition strategy based on (13)C NMR. *Anal. Chem.* **2014**, *86*, 2955–2962. [PubMed]
13. Abedini, A.; Colin, M.; Hubert, J.; Charpentier, E.; Angelis, A.; Bounasri, H.; Bertaux, B.; Kotland, A.; Reffuveille, F.; Nuzillard, J.M.; et al. Abundant Extractable Metabolites from Temperate Tree Barks: The Specific Antimicrobial Activity of *Prunus Avium* Extracts. *Antibiotics* **2020**, *9*, 111.
14. Schmitt, M.; Alabdul Magid, A.; Hubert, J.; Etique, N.; Duca, L.; Voutquenne-Nazabadioko, L. Bio-guided isolation of new phenolic compounds from *Hippocrepis emerus* flowers and investigation of their antioxidant, tyrosinase and elastase inhibitory activities. *Phytochem. Lett.* **2020**, *35*, 28–36.
15. Hammoud Mahdi, D.; Hubert, J.; Renault, J.H.; Martinez, A.; Schubert, A.; Engel, K.M.; Koudogbo, B.; Vissiennon, Z.; Ahyi, V.; Nieber, K.; et al. Chemical profile and antimicrobial activity of the fungus-growing termite strain *Macrotermes bellicosus* used in traditional medicine in the Republic of Benin. *Molecules* **2020**, *25*, 5015.
16. Angelis, A.; Hubert, J.; Aligiannis, N.; Michalea, R.; Abedini, A.; Nuzillard, J.M.; Gangloff, S.C.; Skaltsounis, A.L.; Renault, J.H. Bio-guided isolation of methanol-soluble metabolites of common spruce (*Picea abies*) bark by-products and investigation of their dermo-cosmetic properties. *Molecules* **2016**, *21*, 1586.
17. Hubert, J.; Chollet, S.; Purson, S.; Reynaud, R.; Harakat, D.; Martinez, A.; Nuzillard, J.M.; Renault, J.H. Exploiting the Complementarity between Dereplication and Computer-Assisted Structure Elucidation for the Chemical Profiling of Natural Cosmetic Ingredients: *Tephrosia purpurea* as a Case Study. *J. Nat. Prod.* **2015**, *78*, 1609–1617. [PubMed]
18. Gu, Y.; Jérôme, F. Glycerol as a sustainable solvent for green chemistry. *Green Chem.* **2010**, *12*, 1127–1138.
19. Canton, M.; Hubert, J.; Poigny, S.; Roe, R.; Brunel, Y.; Nuzillard, J.M.; Renault, J.H. Dereplication of natural extracts diluted in glycerin: Physical suppression of glycerin by Centrifugal Partition Chromatography combined with presaturation of solvent signals in 13C-Nuclear Magnetic Resonance spectroscopy. *Molecules* **2020**, *25*, 5061.

20. Louis, A.; Petereit, F.; Lechtenberg, M.; Deters, A.; Hensel, A. Phytochemical characterization of *Rhododendron ferrugineum* and in vitro assessment of an aqueous extract on cell toxicity. *Planta Med.* **2010**, *76*, 1550–1557. [PubMed]
21. Borghesan, M.; Hoogaars, W.M.H.; Varela-Eirin, M.; Talma, N.; Demaria, M. A Senescence-Centric View of Aging: Implications for Longevity and Disease. *Trends Cell Biol.* **2020**, *30*, 777–791.
22. Ryu, S.J.; Oh, Y.S.; Park, S.C. Failure of stress-induced downregulation of Bcl-2 contributes to apoptosis resistance in senescent human diploid fibroblasts. *Cell Death Differ.* **2007**, *14*, 1020–1028.
23. Qiu, J.; Zhang, T.; Zhu, X.; Yang, C.; Wang, Y.; Zhou, N.; Ju, B.; Zhou, T.; Deng, G.; Qiu, C. Hyperoside Induces Breast Cancer Cells Apoptosis via ROS-Mediated NF-κB Signaling Pathway. *Int. J. Mol. Sci.* **2019**, *21*, 131.
24. Pirvu, L.; Stefaniu, A.; Neagu, G.; Albu, B.; Pintilie, L. In Vitro Cytotoxic and antiproliferative activity of *Cydonia oblonga* flower petals, leaf and fruit pellet ethanolic extracts. Docking simulation of the active flavonoids on anti-apoptotic protein Bcl-2. *Open Chem.* **2018**, *16*, 591–604.
25. Rakhshan, R.; Atashi, H.A.; Hoseinian, M.; Jafari, A.; Haghighi, A.; Ziyadloo, F.; Razizadeh, N.; Ghasemian, H.; Nia, M.M.K.; Sefidi, A.B.; et al. The synergistic cytotoxic and apoptotic effect of resveratrol and naringenin on Y79 retinoblastoma cell line. *Anti-Cancer Agents Med. Chem.* **2021**, *21*, 2243–2249.
26. Liu, E.; Liang, T.; Wang, X.; Ban, S.; Han, L.; Li, Q. Apoptosis induced by farrerol in human gastric cancer SGC-7901 cells through the mitochondrial-mediated pathway. *Eur. J. Cancer Prev.* **2015**, *24*, 365–372.
27. Razak, S.; Afsar, T.; Ullah, A.; Almajwal, A.; Alkholief, M.; Alshamsan, A.; Jahan, S. Taxifolin, a natural flavonoid interacts with cell cycle regulators causes cell cycle arrest and causes tumor regression by activating Wnt/β-catenin signaling pathway. *BMC Cancer* **2018**, *18*, 1043.
28. Franco, A.C.; Aveleira, C.; Cavadas, C. Skin senescence: Mechanisms and impact on whole-body aging. *Trends Mol. Med.* **2022**, *28*, 97–109.